

Falling chains as variable mass systems: theoretical model and experimental analysis

Célia A. de Sousa, Paulo M. Gordo and Pedro Costa

*Department of Physics, University of Coimbra, P-3004-516 Coimbra, Portugal**

Abstract

In the present paper we revisit, theoretical and experimentally, the fall of a folded U-chain and of a pile-chain. The model calculation implies the division of the whole system into two subsystems of variable mass, allowing to explore the role of tensional contact forces at the boundary of the subsystems. This justifies, for instance, that the folded U-chain falls faster than the acceleration due to the gravitational force. This result, which matches quite well with the experimental data independently of the type of chain, implies that the falling chain is well described by energy conservation. We verify that these conclusions are not observed for the pile-chain motion.

arXiv:1110.6035v2 [physics.ed-ph] 28 May 2012

*Electronic address: celia@teor.fis.uc.pt

I. INTRODUCTION

The dynamics of variable mass systems has been studied by professors and researches since the 19th century [1], becoming a particular branch within classical mechanics. From now on, applications involving variable mass systems are distributed over a wide range of different areas of knowledge, such as in rocket theory [2], astronomy [3], biology [4], econophysics [5], robotics [6], mechanical and electrical machinery [7] and engineering in general. However, despite these successful applications, even today one can find, in the specialized and/or pedagogical literature, apparent paradoxes that allow for discussions on the fundamentals of the variable mass system dynamics. In practice, we verify that the study of these systems is a challenge for students, and enhances their understanding of laws of dynamics for systems of particles. These are good arguments to the introduction of this theme to students in the scientific areas. To this purpose, ropes or chain systems have been considered as didactic examples, being studied from different points of view. In this context, the published suggestions are carried out by using several procedures, such as the concept of momentum flux [8, 9], the generalization of Newton's second law [10], analytical methods [11], and numerical simulations [12]. Some of these methodologies are adequate frameworks for beginning students of physics [13].

In the present paper, we consider two well known examples of such systems: a folded chain initially suspended from a rigid support by the two ends placed closed together, and then one of the ends is released; and a chain, part of which is hanging off the edge of a smooth table. We refer briefly to these systems as U-chain and pile-chain [14]. The example of the pile-chain is equivalent to a pile of chain falling through a smooth hole. However, we prefer to consider here the pile-chain falling off from the edge of a support because it is easier to solve technical difficulties in the experimental procedure.

Recent experimental observations that the free end of the U-chain falls faster than g [12, 15, 16] have contributed to an increasing interest on the behavior of systems such as ropes and chains. Such a behavior admits that the falling chain is a conservative system. For completeness and comparative purposes, we also include the model calculation where the energy conserving assumption is not considered *a priori*. In this case the acceleration of the falling arm of the U-chain is g .

In the pile-chain configuration, the hypothesis of conservation of mechanical energy leads

to the value $g/2$ for the acceleration of the chain tip [10]. If the energy conserving scenario is not assumed *a priori*, the value $g/3$ is obtained [1].

As already referred by other authors [11], there are significant differences between the behavior of chain systems in the two configurations. Whereas in the falling U-chain it is possible to obtain a link-by-link mass transfer at the fold of the chain, such a behavior is difficult to realize in a real chain falling from a resting heap through a hole. In fact, it is very difficult to get a well arranged pile in order to allow for a steady motion. So, it is tricky to confirm experimentally which model is more reliable to describe such systems in this configuration. Some authors also refer to an additional complexity which consists in the lift above the platform before the fall of the chain, a feature justified by the energy conserving assumption as will be discussed later.

Newton's second law for variable mass systems have been successfully applied to chains and ropes, independently of the model assumption, i.e., by either considering or not the energy conservation approach [10]. The method, here included for the sake of completeness, considers the whole system divided into two subsystems of variable mass. The motion is one-dimensional, and the forces at the boundary of the two subsystems, one of which is at rest, can be calculated. This explains, for instance, why the acceleration of the falling chain is larger than g in the U-chain when the energy conserving approach is assumed.

A special attention is dedicated to the pile-chain configuration. As already referred, some aspects of this problem have been solved in the literature by two distinct approaches. Our main purpose is to discuss the two solutions $a = g/3$ and $a = g/2$, trying to confront these theoretical results with the experimental data. Bearing in mind the important role played by tensional contact forces, we also show that the analysis of the variable mass system, as a redistribution of mass between the two subsystems, is reliable to study that tension. We remind that some treatments analyse the problem using energy conservation only, without deriving equations of motion.

We include in section 2 a summary of the methodology used to study variable mass systems, and in section 3 we present the experimental setup. Two illustrative examples are studied theoretical and experimentally in sections 4 and 5. Section 6 contains the concluding remarks.

II. THEORETICAL BACKGROUND: NEWTON'S SECOND LAW FOR VARIABLE MASS SYSTEMS

The equations of motion of the falling chains can be obtained by considering a closed one-dimensional system of constant total mass composed by two open subsystems which exchange mass. So, the systems considered in this paper have the characteristics indicated below.

- (i) The whole system, a constant mass one, can be divided into two (variable mass) subsystems I and II with masses m_I and m_{II} , respectively. To the whole system the traditional Newton's second law, $F = (m_I + m_{II}) a_{\text{cm}}$, where a_{cm} is the acceleration of the center of mass, or $F = dp/dt$, in terms of linear momentum, are valid.
- (ii) One of the subsystems (I) is moving with velocity v , and the other (II) is at rest.
- (iii) The velocity of the mass being transferred between the subsystems is $u = v$.

Under these assumptions two expressions can be obtained for each subsystem (see [10] for details)

$$F^{(I)} = \frac{d}{dt} (m_I u) - u \frac{dm_I}{dt}, \quad (1)$$

and

$$F^{(II)} = \frac{d}{dt} (m_{II} v) - u \frac{dm_{II}}{dt}, \quad (2)$$

where $u dm_{II}/dt$ ($u dm_I/dt$) is the rate at which momentum is carried into (away) the system of mass m_{II} (m_I) — “momentum flux”.

As both equations (1) and (2) have a common generic structure, hereafter the symbols I and II are dropped allowing to write Newton's second law for variable mass systems in the form

$$\frac{dp}{dt} = F + u \frac{dm}{dt}, \quad (3)$$

where m is the instantaneous mass, $p = m v$ its linear momentum, and F is the net external force acting upon the variable mass system.

III. EXPERIMENTAL SETUP

The experimental measurements were performed using three chains: one “ball chain” and two sizes, medium and large, of normal “linked chains”. The ball chain consists of stainless-steel identical segments made from rods and spheres attached to each other. The two loop chains are made of torus-shaped links. The dimensions of the torus-shaped links of the medium (large) linked chain are: length 11 mm (20 mm) and width 18 mm (24 mm). Other characteristics of the chains are given in table I.

Chain	l(m)	m(kg)	λ (kg/m)	Number of links
ball chain	1.830(1)	0.0395(1)	0.0216(1)	419
medium loop chain	1.859(1)	0.1860(1)	0.1001(1)	115
large loop chain	1.738(1)	0.4029(1)	0.2318(1)	99

TABLE I: Characteristics of chains used in the experiments.

The experimental setup is based on the force sensor from Pasco model CI-6537 (maximum force of 50 N), that is usually available in most educational laboratories. The signal from the force sensor is monitored using a ScienceWorkshop interface, model 750 also from Pasco, connected to a personal computer, that makes use of DataStudio (version 1.9.7r12) software to control the data acquisition. The typical time duration of the events that we are investigating is of the order of 1 second or less. The rate acquisition signals of 1 kHz or higher is sufficient to reveal the details of the dynamics during the experiment. We acquired the signals at 1, 2, 4 and 10 kHz, which gave similar information in all cases except in the number of data points to manipulate. We have also used a photogate head, model ME-9204B from Pasco, to define the important and critical instant $t = 0$.

For the U-chain experiment, one of the ends of the chain was attached to the hook of the fixed force sensor and the other end was released from the same height. The system is in vertical position and the sensor measures the net force by the chain on sensor’s hook.

For the pile-chain experiment two different devices were used: (A) a flat polished squared wood table with 21.5 cm of length, fixed to the force sensor, from which the pile-chain falls down; and (B) a ceramic ashtray of diameter 8.58 cm, with lateral U-shaped overture of width approximately 2.5 cm, also fixed to the force sensor. In both cases, a special

accessory was used to attach the devices to the force sensor. The beginning of the chain's fall was monitored by the photogate sensor which was placed near the border of the table (overture of the ashtray).

IV. ANALYSIS OF THE U-CHAIN

A folded uniform chain with length l and mass per unity of length λ is considered. In figure 1 we illustrate the configuration of the system at $t = 0$ and $t \neq 0$, where x is a generic position of point B. As illustrated, the axis x points downwards and, for convenience, the system is divided into two subsystems I and II (see figure 1 and table II).

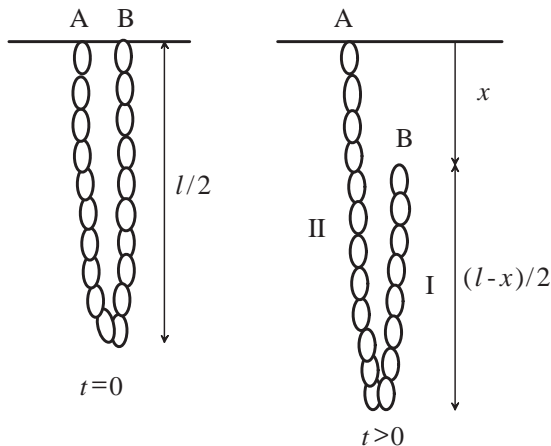


FIG. 1: Scheme of the U-chain configuration.

A. Energy conserving assumption

We start by considering that the mechanical energy of the U-chain is conserved [11, 12, 15]. Within this model assumption, the acceleration of the falling chain is not known, neither are the tension forces indicated in table II. Consequently, it is not convenient to start the resolution of the system by using Newton's second law for constant or variable mass systems.

The variation of kinetic and potential energies are easily calculated and, from the conservation of energy $\Delta E = 0$ we obtain [17]

$$\frac{\lambda}{4}(l-x)v^2 - \frac{\lambda}{4}gx(2l-x) = 0. \quad (4)$$

System	m	p	F	u	udm/dt
I	$\frac{\lambda}{2}(l-x)$	$\frac{\lambda}{2}(l-x)v$	$\frac{\lambda}{2}(l-x)g + T_1(x)$	v	$-\frac{\lambda}{2}v^2$
II	$\frac{\lambda}{2}(l+x)$	0	$\frac{\lambda}{2}(l+x)g + T(x) + T_2(x)$	v	$\frac{\lambda}{2}v^2$
I+II	λl	$\frac{\lambda}{2}(l-x)v$	$\lambda l g + T(x)$	—	—

TABLE II: Summary of the relevant physical quantities for the U-chain. See the text for notation.

Eliminating $v^2(x)$ from the last equation, we find

$$v^2(x) = gx \frac{2l-x}{l-x}. \quad (5)$$

The acceleration of the falling arm of the chain can be obtained directly from this equation by applying the following mathematical procedure:

$$a = \frac{dv}{dt} = \frac{dv}{dx} \frac{dx}{dt} = \frac{1}{2} \frac{dv^2}{dx}, \quad (6)$$

giving

$$a = g + \frac{g}{2} \frac{x(2l-x)}{(l-x)^2} = g + \frac{v^2}{2(l-x)}. \quad (7)$$

The application of Newton's second law to the whole system, for instance in the form $F = dp/dt$, allows for the tension, $T(x)$, acting on the chain by the support (see table II). In fact, we can write

$$\frac{d}{dt} \left(\frac{\lambda}{2}(l-x)v \right) = \lambda l g + T(x). \quad (8)$$

We substitute (5) and (7) into (8) and find

$$T(x) = -\frac{\lambda}{2} g(l+x) - \frac{\lambda}{4} gx \frac{2l-x}{l-x}, \quad (9)$$

where the minus sign indicates that this force acts upward, as it must be.

It is instructive to rewrite this equation in the form

$$T(x) = -\frac{\lambda}{2} g(l+x) - \frac{\lambda}{4} v^2, \quad (10)$$

showing that this tension force results from the instantaneous “weight” of the chain, i.e., from the weight of the static side of the chain (II) at a given instant, and an additional “dynamic weight” which depends on the velocity of the falling side (I).

The contact at the bottom provides a tension force $T_1(x)$ that can be obtained by applying Newton’s second law (3) for subsystem I. In fact, for this subsystem one has (see table II and figure 1)

$$m = \frac{\lambda}{2}(l - x), \quad p = \frac{\lambda}{2}(l - x)v, \quad \text{and} \quad u \frac{dm}{dt} = -\frac{\lambda}{2}v^2, \quad (11)$$

allowing for

$$T_1(x) = \frac{\lambda}{4}gx \frac{2l - x}{l - x}. \quad (12)$$

We point out that this expression for $T_1(x)$ can be rewritten in the form $T_1(x) = \lambda v^2/4$, result that can also be obtained using the Lagrangian formalism [11].

The downward tension $T_1(x)$ in the chain on the falling side pulls the chain down in addition to the gravitational force. So, with this methodology, the tension at the fold comes naturally.

The same procedure applied to subsystem II allows for the tension $T_2(x) = -T_1(x)$, satisfying Newton’s third law.

To compare the model calculations with the experimental results we integrate (5). To avoid the complexity, which comes from the solution of $x(t)$ in terms of elliptic integrals, we compute this function of time numerically. With this procedure we obtain $x = x(t)$ that, together with (9), allows to attain $T = T(t)$.

B. Free fall assumption

Now, the energy conserving assumption is not considered *a priori*. Instead, we assume that the falling part of the chain (subsystem I) falls with an acceleration g , as in free fall [17]. This model assumption presented in [10] with other geometry is briefly presented here by completeness and comparative purposes.

So, by applying (3) to subsystem I (see table 2 and figure 1) we conclude that $T_1(x) = 0$.

An analogous procedure applied to subsystem II, together with the condition $T_2(x) = -T_1(x) = 0$, allows to obtain the tension at the support

$$T(x) = -\frac{\lambda}{2}g(l+x) - \frac{\lambda}{2}v^2. \quad (13)$$

The expression of the squared velocity as a function of x can be calculated by using equation (6) with $a = g$, allowing for

$$v^2(x) = 2gx. \quad (14)$$

Finally, from the two last equations we obtain

$$T(x) = -\frac{\lambda}{2}gl \left(1 + 3\frac{x}{l}\right). \quad (15)$$

To compare this model calculation with the experimental results the well known solution $x(t) = 1/2gt^2$ is used to obtain the tension

$$T(t) = -\frac{\lambda}{2}gl \left(1 + \frac{3}{2}\frac{g}{l}t^2\right). \quad (16)$$

C. Comparison with the experimental results

The theoretical calculations obtained in the previous subsections are going to be compared with the experimental results. We start releasing the ball type chain. In figure 2 we present the typical signal from the force sensor, measuring the force by the falling chain in the sensor. Similar curves were observed for the other two loop chains, except in some details such as the magnitude of the measured force due to different weight of the chains. The represented values of the force are negative because of the convention signal of the sensor: it is positive (negative) when there is a compression (distension) of the sensor.

For $t = 0$, the value observed in the sensor corresponds to half of the weight of the ball chain, $T_0 = -0.193$ N, and the fall of the chain occurs in approximately 0.5 s, when maximum value for the tension force is achieved. The behavior of the tension $T(t)$ for $t > 0.5$ s reflects the ricochet effect of the chain in the sensor. The maximum value of the tension achieved at the end of the fall is larger than 50 times the chain's weight. This agrees with the energy conserving assumption for this system, which predicts a very high velocity (see (5)) of the chain at the end of the fall and, consequently, a very strong variation of T at the end of the movement. For instance, $T/T_0 = 51.9$ at $x/l = 0.99$ in this model assumption, whereas in the free fall assumption $T/T_0 = 4$ at $x = l$ (see (15)). We remember that the

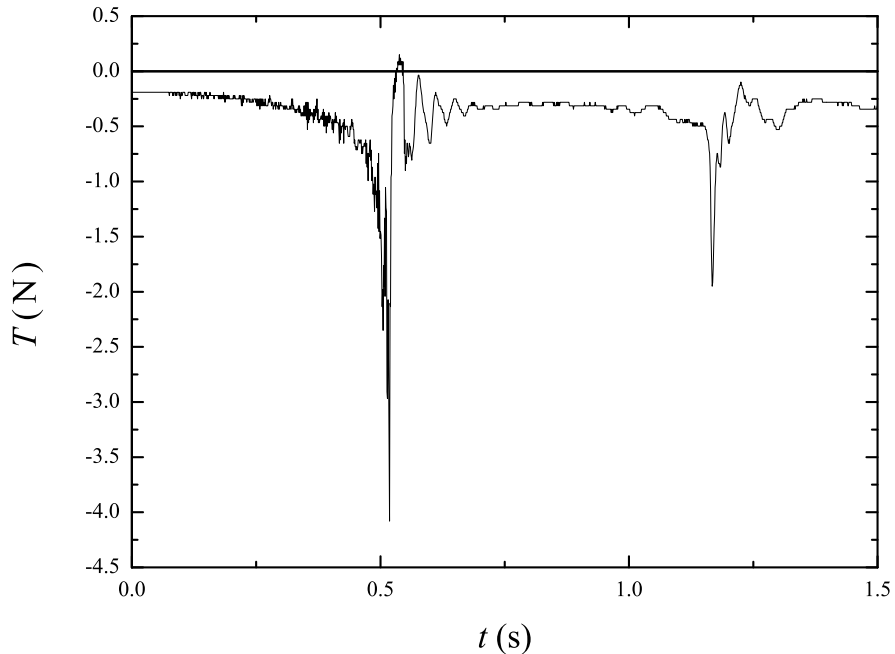


FIG. 2: Tension at the fixed end of the chain as a function of time for the ball chain.

force sensor reads the instantaneous “weight” of the chain, which is larger than the weight of the chain actually at rest at a given instant.

In figure 3, the theoretical results of the tension $T(t)$ as a function of t are plotted during the fall of the chain together with the experimental results, for the cases: (a) ball chain, (b) medium loop chain, and (c) large loop chain. As referred in subsection 4.1, the theoretical curves in the energy conserving approach have been obtained numerically. The observed fluctuations in the value of T are mainly due to the discrete shape of the chains especially in the case of loop chains as can be seen in figure 3. A larger loop chain corresponds to higher amplitude of these fluctuations (notice the difference of scale in the three cases). It can also be seen that the fall time for all chains are quite identical, because of the similarity of the length of the chains (see table I); the shorter time is observed for the large loop chain, the one with the shortest length (about minus 10 cm). For the large and medium loop chains, the maximum values of T achieved (not represented in the figure) are several orders of magnitude higher than their weight. The correct value could not be determined precisely due to the limit of 50 N for the maximum force of the sensor.

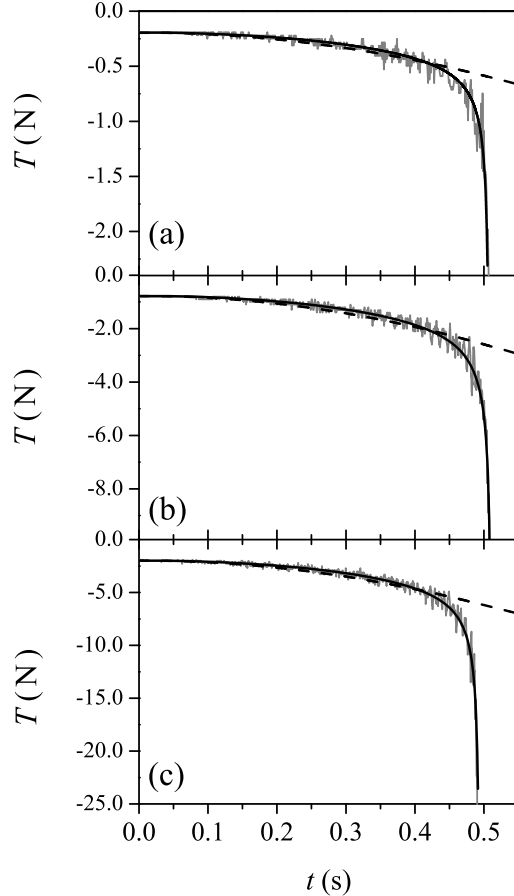


FIG. 3: Tension at the fixed end of the chain as a function of time for: (a) ball chain, (b) medium loop chain, and (c) large loop chain. The solid (dashed) curve represents the theoretical result obtained by energy conserving (free fall) assumption.

It can be seen that the theoretical result given by the solid curve and the experimental data fit quite well, and we can conclude that the dynamics of the falling chain is very well described by the conservation of energy assumption, independently of the type of chain. This is explained by the continuous interference (no broken contacts) at the fold of the chains during the motion. Consequently, the acceleration of the moving part of the chain is higher than g at the end of the movement. The falling chain is divided into two subsystems: the almost motionless part attached to the support and the moving part. The falling chain lowers its potential energy on the account of the kinetic energy of the continuously shorter part of the chain. Because the mass of the latter decreases, its velocity grows significantly. We remember that, as it was reported early [16], if the initial distance between the ends of

the chain is moderated, the contribution to the kinetic energy from the horizontal motion is a small fraction of that due to the vertical motion, and the system can appropriately be treated in the limiting one-dimensional motion. We can conclude that real chains behave like a flexible and inextensible conservative system.

V. ANALYSIS OF THE PILE-CHAIN

Now we consider the fall of a pile-chain from the edge of a platform. One end of the chain falls and pulls the chain after it in a steady motion (see figure 4). The chain starts moving from rest at $x = 0$ and the x axis points downward. This geometry is equivalent to the fall of a pile of chain placed just above a hole in a platform. In fact, both problems reflect the same physical reality, however, the first case is more easily implemented by normal pieces like a flat platform or an ashtray. As already referred, some aspects of this problem have been solved in the literature by considering two scenarios. Our purpose is to discuss both solutions for the force on the platform, trying to confront the results with experimental data.

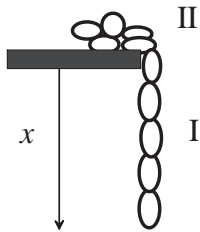


FIG. 4: Scheme of the falling pile-chain.

A. Energy conserving assumption

We consider that the chain is a one-dimensional system and we start with the assumption of conservation of mechanical energy. The acceleration of the falling chain is not known, as well as the force $N(x)$ acting on the chain by the platform.

Referring to figure 4, we see that from the conservation of energy we obtain

$$\frac{1}{2} \lambda x v^2 - \frac{1}{2} \lambda g x^2 = 0, \tag{17}$$

System	m	p	F
I	λx	$\lambda x v$	$\lambda x g + T_1(x)$
II	$\lambda(l - x)$	0	$\lambda(l - x)g + T_2(x) + N(x)$
I+II	λl	$\lambda x v$	$\lambda l g + N(x)$

TABLE III: Summary of the relevant physical quantities for the pile-chain. See the text for notation.

which gives the square of the velocity v^2 in terms of x :

$$v^2(x) = g x. \quad (18)$$

The acceleration of the falling rope can be obtained:

$$a = \frac{dv}{dt} = \frac{1}{2} \frac{dv^2}{dx} = \frac{g}{2}. \quad (19)$$

Now, we apply Newton's second law, for instance in the form $F = dp/dt$, to the whole system of constant mass λl .

The net external forces acting on this system are the downward gravity and the normal force by the platform, $N(x)$, allowing for the equation of motion (see table III)

$$\frac{d}{dt}(\lambda x v) = \lambda l g + N(x). \quad (20)$$

Straightforward calculation, which includes the substitution of v and a in the previous equation, provides the total force by the platform on the chain

$$N(x) = -\lambda \left(l - \frac{3}{2} x \right) g, \quad (21)$$

where the minus sign indicates that this force acts upward, as it must be. This equation also shows that $N(x) = 0$ when $x = 2l/3$, indicating the domain of validity of the previous equation in the interval $0 \leq x \leq 2l/3$.

As in the previous example, the application of Newton's second law to the variable mass system I (II) allows the calculation of the tension $T_1(x)$ ($T_2(x)$) at the boundary of subsystem I (II). In fact, for subsystem I one has (see table III and figure 4)

$$m = \lambda x, \quad p = \lambda x v, \quad \text{and} \quad u \frac{dm}{dt} = \lambda v^2. \quad (22)$$

Using (22) in (3) with F given from table 3, leads to

$$T_1(x) = -\lambda x g/2 = -\lambda v^2/2. \quad (23)$$

With this procedure the tension at the boundary of the subsystems comes naturally.

To compare with the experimental results, we calculate the expression for $N(t)$ by inserting the equation of motion $x = \frac{1}{4} g t^2$ into (21), and thus

$$N(t) = -\lambda l g \left(1 - \frac{3g}{8l} t^2 \right). \quad (24)$$

We notice that the problem at hand has four unknowns: the acceleration a , the normal $N(x)$, and the tension forces $T_1(x)$ and $T_2(x)$ acting through the boundary of the subsystems. As $T_1(x)$ and $T_2(x)$ satisfy Newton's third law, we have, effectively, three unknowns to be determined by three equations: the law of conservation of energy, and for instance, Newton's second law applied to the whole system and Newton's second law for variable mass system I or II.

B. Tait-Steele solution

Now, we consider that mechanical energy is not conserved *a priori*. As the number of unknowns holds, the system is undetermined. To make the equations determined while preserving their simplicity, some conditions must be imposed.

Tait and Steele solve the problem by using Newton's second law in the form [18]

$$\frac{d}{dt}(\lambda x v) = \lambda x g. \quad (25)$$

This equation can be written as a first-order linear equation in v^2

$$v x \frac{dv}{dx} + v^2 = x g. \quad (26)$$

The solution of this equation is

$$v(x) = \left(\frac{2}{3} g x \right)^{1/2}, \quad (27)$$

allowing for the well known result $a = g/3$.

However, the falling chain is a variable mass system for which Newton's second law $F = dp/dt$ is not *a priori* valid, unless the following conditions are imposed

$$u = 0, \quad \text{and} \quad T_1(x) = 0, \quad (28)$$

i.e., particles enter/leave the variable mass system with zero velocity, and there is no interference between adjacent links in the boundary of both subsystems.

Alternatively, it is also possible to obtain (25) by applying Newton's second law to subsystem I (see (3) and table III), with the more realistic condition $u = v$, if we also impose an *empirical* condition on T_1 , i.e.,

$$u = v, \quad \text{and} \quad T_1(x) = -\lambda v^2. \quad (29)$$

With these conditions, the effect of the upward tension T_1 is canceled by the “momentum flux”, $u \, d m / d t$, carried away from subsystem I.

In reality, we must consider $u = v$, and the tension $T_1(x)$ is undetermined. Consequently, Newton's second law (see (3)) applied to subsystem I allows for

$$a = g + \frac{T_1(x)}{\lambda x}. \quad (30)$$

This problem is absent in the U-chain description when the conservation of energy is not considered *a priori*, because the condition $a = g$ for the acceleration of the falling chain is assumed. This provides the extra equation necessary to solve the problem, and $T_1(x) = 0$ comes naturally.

Finally, to test the reliability of the solution $a = g/3$, we are going to obtain the force on the chain by the platform, $N(t)$, to be compared with the experimental data.

To this purpose, applying Newton's second law to the whole constant mass system, we write

$$\frac{d}{dt}(\lambda x v) = \lambda l g + N(x). \quad (31)$$

Comparing (31) and (25), we find now the expression

$$N(x) = -\lambda g(l - x), \quad (32)$$

which can be expressed in terms of time:

$$N(t) = -\lambda l g \left(1 - \frac{1}{6} \frac{g}{l} t^2 \right). \quad (33)$$

C. Comparison with the experimental results

To perform this experiment we have elaborated two configurations: (A) a flat polished squared wood table and (B) a ceramic ashtray with lateral U-shaped overture from which the chain falls down.

The instant $t = 0$ has been determined by a photogate sensor, which was placed near the border of the table (overture of the ashtray). This configuration enables us to identify the critical instant of the beginning of the chains fall which is difficult to check otherwise.

In figure 5, we show the behavior of the normal N for the ball chain in the experimental configuration setup (A). The theoretical results obtained by the energy conserving approach (24) and by the Tait-Steele solution (33), represented by the solid and dashed curves, respectively, are also shown.

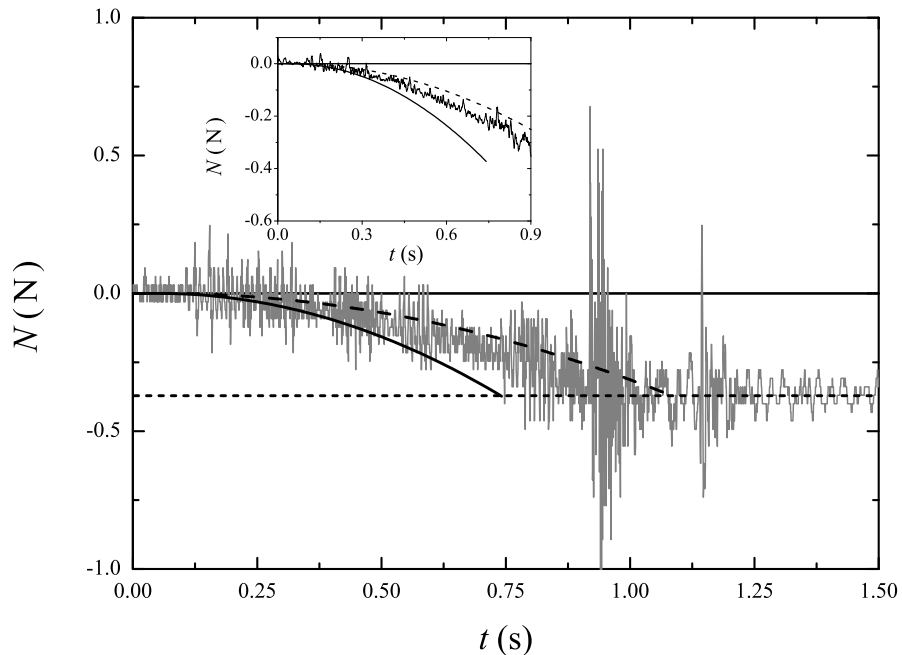


FIG. 5: Normal force as a function of time for the ball chain on the platform. The theoretical results for energy conserving approach (solid curve) and for Tait-Steele solution (dashed curve) are also included. Inset: Filtered signal. The signal is smoothed by averaging over an interval of 10 ms.

At $t = 0$ the value of the normal force N is, of course, the weight of the chain, re-scaled to $N = 0$. Consequently, after the fall of the chain, the absolute value of N represents its weight (horizontal dashed line). The fall of the entire chain occurs in approximately 0.9 s.

As can be seen in figure 5, instead of the continuous quadratic decrease in the normal, $N(t)$, we observe relatively large fluctuations in the force signal during the fall. These fluctuations are a natural consequence of the discrete nature of the chain and must be associated with the collisions of the links with the border of the table. This effect is clearly reinforced with both loop chains as we will see later, as a consequence of a more pronounced discrete nature of the systems. The amplitude of the fluctuations increases with time and the frequency of the peaks raises, as well, due to the increase of the frequency of the collisions. In the case of the ball chain, this effect is less pronounced since the system is almost a “continuous system” as a result of the small size and mass of the spheres that compose the chain. The “hidden” ideal force N can then be revealed by using a numerical filtering procedure, which takes the average force value during 10 ms (see figure 5, inset).

By comparing the experimental results with the theoretical curves, we observe that the dynamics of the ball chain is not adequately described by any of the two models. Particularly, the solid curve for the energy conserving assumption diverges significantly from the experimental data. From the point of view of this energy conserving approach, and according to (21), it was expected a normal force $N = 0$ (in the figure N is equal to the weight of the chain due to the re-scale done) when $x = 2l/3$, which is only observed during the experiment for $x \approx l$. In fact, just before the total fall from the platform, the very last small portion of the chain suffers a jump from the table. When the experiment is repeated using the configuration setup (B), a quite similar behavior is observed for this chain. These features suggest that the ball chain can provide the “ideal” framework to discuss the validity of the theoretical model assumptions. As will be seen below, when the experiments are made with the loop chains, significant differences between the data of the two setups are observed.

The main conclusion is that the actual experimental configuration is not well described by the one-dimension motion of the pile-chain either assuming energy conservation or not and, consequently, the real chains do not act more like a perfect flexible, inextensible rope as it was observed in the U-chain experiments. In practice, it is not technically possible to accommodate the static part of the chain in a “single point”. So, in order to obtain a steady motion of the falling chain, the system must spread over a finite area, which introduces

features not included in the theoretical model assumptions. Indeed, due to the finite size and width of the chain, the contribution to the kinetic energy from the horizontal motion of the chain over the table is a significant fraction of that due to the vertical motion. To treat correctly this system the full two-dimensional motion of the pile-chain has to be considered, which is a difficult mathematical task. Furthermore, it is also impossible to eliminate some dissipative mechanisms such as friction or interferences, and collisions between the links of the chain.

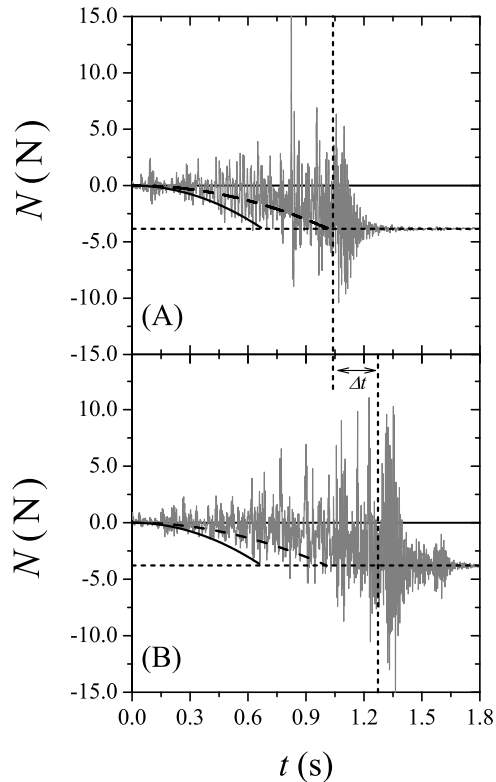


FIG. 6: Comparison of the normal as a function of time for the large loop chain in the platform (A) and in the ashtray (B). The theoretical results for energy conserving model (solid curve) and for Tait-Steele solution (dashed curve) are also included.

The dissipative mechanisms are, of course, strongly dependent on the experimental apparatus. This is illustrated in figure 6 where a significant difference in the results for both configuration setups (A) and (B) for the large loop chain are shown. Of course, in this case the experimental result is also not described by any of the two models. As a consequence of

the loop structure of this chain, the collisions between the links are present and a concomitant lost of energy is associated with this phenomenon. There are also external dissipative forces like friction over the border of the table (configuration setup (A)) or collisions with the borders of the overture of the ashtray (configuration setup (B)), which represents a significant loss of mechanical energy. In the case of the setup (B), once the number of collisions is expected to be higher, the energy lost must be also more pronounced. This description agrees well with the difference in time, Δt , that has been observed for the large loop chain in the configuration setups (A) and (B): the longer fall time observed in the configuration setup (B) is associated with a higher loss of energy and, consequently, a reduction in the speed of the chain. We notice that $\Delta t \approx 0.25$ s and this value represents an increase of about 25% in the fall time. For the medium loop chain we have observed similar results (not shown) as for the large loop chain.

VI. SUMMARY AND CONCLUSIONS

The theoretical method suggested allows the discussion of falling chains as variable mass systems. The whole system is divided into two subsystems of variable mass. With this procedure the tension at the boundary of the subsystems comes naturally when the Newton's second law for variable mass systems is applied.

The theoretical results provided by the energy conserving assumption have the following characteristics:

- in the falling U-chain, the contact at the bottom results in a downward tension force $T_1 = \lambda v^2/4$, pulling the falling part with an acceleration larger than g ;
- in the pile-chain, the contact at the top originates an upward tension force $T_1 = -\lambda v^2/2$, slowing down the falling part with an acceleration ($g/2$) smaller than g .

The model calculation when the energy conservation is not assumed *a priori* allows the following conclusions:

- in the U-chain, it is assumed that $a = g$ and $u = v$, allowing for $T_1 = 0$;
- in the pile-chain, the acceleration is undetermined, unless it is assumed that $T_1 = 0$ ($T_1 = -\lambda v^2$) and $u = 0$ ($u = v$), which allows for $a = g/3$.

As already verified by other authors, the experimental data for the U-chain shows a good convergence with the energy conserving approach, independently of the type of chain. There exists continuous interference (no broken contact) during the motion and, consequently, the dissipative effects of explicit collisions, even in a discrete chain, are negligible. In addition, one-dimensional model is a good approach for this configuration.

To model the pile-chain motion two devices have been used: a flat platform and a ceramic ashtray. We observe that the ball chain has a similar behavior in both experimental apparatus, showing that it constitutes an “ideal” system to this type of analysis. The measured data with this chain shows that the system is not well described by one-dimensional motion only. For the loop chains dissipative mechanisms like friction and collisions between the loop and the borders of the table and ashtray are present and must be taken into account.

The experience with the ball chain falling from the platform is particularly important, showing that it provides the best situation between the ideal case and the experimental constraints, but it reveals that the system can not be modeled by one-dimensional motion alone.

Acknowledgements

Work supported by F.C.T. and Physics Department.

-
- [1] Cayley A 1857 On a class of dynamical problems *Proc. R. Soc. London* **8** 506–511
 - [2] Meirovitch L 1970 General motion of a variable-mass flexible rocket with internal flow *J. Spacecr. Rockets* **7** 186–195; Tran T and Eke F O 2005 Effects of internal mass flow on the attitude dynamics of variable mass systems *Adv. Astronaut. Sci.* **119** (Issue Suppl.) 1297-1316
 - [3] Kayuk Ya F and Denisenko V I 2004 Motion of a mechanical system with variable mass-inertia characteristics *Int. Appl. Mech.* **40** 814–820
 - [4] Canessa E 2007 Modeling of body mass index by Newtons’s second law *Jour. Theor. Biology* **248** 646–656
 - [5] Canessa E 2009 Stock market and motion of a variable mass spring *Physica A* **388** 2168–2172
 - [6] Djerassi S 1998 An algorithm for simulation of motions of variable mass systems *Adv. Astronaut. Sci.* **99** 461–474
 - [7] Cveticanin E 2010 Dynamics of the non-ideal mechanical systems: A review *J. Serbian Soc.*

for Comp. Mech. **4** 75–86

- [8] Siegel S 1972 More about variable mass systems *Am. J. Phys.* **40** 183–5
- [9] de Sousa C A 2002 Nonrigid systems: mechanical and thermodynamic aspects *Eur. J. Phys.* **23** 433–440
- [10] de Sousa C A and Rodrigues V H 2004 Mass redistribution in variable mass systems *Eur. J. Phys.* **25** 41–49
- [11] Wong C W and Yasui K 2006 Falling chains *Am. J. Phys.* **74** 490–496
- [12] Tomaszewski W, Pieranski P, and J.-C. Géminard J C 2006 The motion of a freely falling chain tip *Am. J. Phys.* **74** 776–783
- [13] de Sousa C A 2012 Atwood’s machine as a tool to introduce variable mass systems *Phys. Ed.* **47** 169–173 (arXiv:1110.6022v1 (physics.ed-ph))
- [14] Grewal A, Johnson P and Ruina A 2011 A chain that speeds up, rather than slows, due to collisions: How compression can cause tension *Am. J. Phys.* **79** 723–729
- [15] Hamm E and Géminard J C 2010 The weight of a falling chain, revisited *Am. J. Phys.* **78** 828–833
- [16] Calkin M G and March R H 1989 The dynamics of a falling chain: I *Am. J. Phys.* **57** 154–157
- [17] Marion J B and Thornton S T 1995 *Classical Dynamics* 4th ed. (Saunders, Fort Worth, TX) example 9.2 of sec. 9.3 pp. 338–340
- [18] Tait P G and Steele W J 1900 *A Treatise on Dynamics of a Particle* 7th ed. (London: Macmillan) pp. 334–335